Hindawi
International Journal of Chemical Engineering
Volume 2023, Article ID 9342174, 11 pages
https://doi.org/10.1155/2023/9342174

Research Article

Effects of Thermodiffusion and Chemical Reaction on Magnetohydrodynamic-Radiated Unsteady Flow Past an Exponentially Accelerated Inclined Permeable Plate Embedded in a Porous Medium

B. Prabhakar Reddy, M. H. Simba, and Alfred Hugo

Department of Mathematics and Statistics, CNMS, The University of Dodoma, P. O. Box 338, Dodoma, Tanzania

Correspondence should be addressed to B. Prabhakar Reddy; prabhakar.bijjula@gmail.com

Received 7 March 2022; Revised 1 June 2022; Accepted 12 April 2023; Published 25 April 2023

Academic Editor: Pedro Castano

A finite difference computational study is conducted to assess the influence of thermodiffusion and chemical reaction on unsteady free convective radiated magnetohydrodynamic flow past an exponentially accelerated inclined permeable plate embedded in a saturated porous medium of uniform permeability with variable temperature and concentration. The governing nondimensional set of coupled nonlinear partial differential equations with related initial and boundary conditions are solved numerically by using the accurate and efficient DuFort–Frankel's explicit finite difference method. The physical features of fluid flow, heat, and mass transfer under the influence of the magnetic field, angle of inclination, plate acceleration, radiation, heat source/sink, thermodiffusion, chemical reaction, and time are scrutinized by plotting graphs and then discussed in detail. It was found that the effective magnetic field and angle of inclination tend to decline the fluid motion, whereas the reverse result is detected by increasing the porosity parameter and plate acceleration. The velocity and temperature of the fluid lessen with increasing the radiation parameter. The effect of thermodiffusion raises the fluid velocity and concentration, whereas a chemical reaction has the opposite impact. The Nusselt number increases with increasing the radiation parameter and time. Increasing chemical reaction and time causes to improve the Sherwood number. This kind of problem finds momentous industrial applications such as food processing, polymer production, inclined surfaces in a seepage flow, and design of fins.

1. Introduction

The study of thermal radiation effect on the boundary-layer flow with heat and mass transfer is of immense curiosity due to its significant applications in many industrial and space technologies such as glass production and furnace design, space vehicle, propulsion systems, comical flight aerodynamics rocket, and spacecraft re-entry aerodynamics which operate at high temperatures, ship compressors, and solar radiation. Due to these imperative applications, the researchers [1, 2] analyzed the radiation effect on MHD flow under different conditions. Pattnaik et al. [3] discussed radiation and mass transfer effects on MHD-free convective flow through a porous medium past an exponentially accelerated vertical plate with variable temperature. Subsequently, the significant research investigations [4–8] richly scrutinized the effect of radiation by considering dissimilar fluids under different circumstances. Veera Krishna et al. [9] recently studied radiation effects on free convective rotating MHD flow through a saturated porous medium over an exponentially accelerated plate by considering Hall and ion slip effects. Veera Krishna et al. [10] examined radiation effects on the MHD flow of second-grade fluid through a porous medium over a semi-infinite vertical stretching sheet. Veera Krishna et al. [11] discussed radiation absorption effects by considering the convective flow of MHD nanofluids through a vertically travelling absorbent plate. Veera Krishna et al. [12] analyzed thermal radiation effects

on oscillatory rotating MHD micropolar liquid in the presence of chemical reaction and Hall and ion slip effects.

The chemical reaction is the process by means of which one set of chemical substances is transported into another. In addition, the process of chemical reaction takes place between the fluid and foreign mass. The study of heat and mass transfer problems by considering chemical reaction effects into account originate plentiful applications in several chemical and hydrometallurgical industries, such as the production of glassware and ceramics, food processing, undergoing endothermic or exothermic chemical reaction, and catalytic chemical reactors, etc. Sugunamma et al. [13] studied inclined magnetic field and chemical reaction effects on flow over a semi-infinite vertical porous plate through a porous medium. Ali et al. [14] presented chemical reaction effects on heat and mass transfer-free convection MHD flow past a vertical plate embedded in a porous medium. Mythreye et al. [15] analyzed chemical reaction effects on unsteady convective MHD heat and mass transfer past a semi-infinite vertical permeable moving plate in the presence of heat absorption. Seth and Sarkar [16] studied hydromagnetic natural convection flow with an induced magnetic field and nth-order chemical reaction of a heat-absorbing fluid past an impulsively moving vertical plate with ramped temperature. Tripathy et al. [17] discussed the chemical reaction effect on MHD-free convective surface over a moving vertical plate through a porous medium. Agarwalla and Ahmed [18] investigated chemical reaction effects on MHD flow past an inclined plate with variable temperature and plate velocity embedded in a porous medium. Subsequently, the research studies [19-23] considered dissimilar fluids to discuss the impact of chemical reaction under different conditions. Recently, Veera Krishna et al. [24, 25] studied a chemical reaction impact by considering the MHD flow of Casson hybrid nanofluid and heat-generating/absorbing second-grade fluid.

In many studies mentioned earlier, the consequence of thermodiffusion on fluid transport may be ignored based on a smaller order of enormity. However, an exciting macroscopically physical phenomenon in fluid mechanics known as thermodiffusion (Soret) effects has significance in thermal diffusion processes. When the combined buoyancy effects happen due to the variation of density with temperature under natural convection, the diffusion of species will be influenced by the temperature. Mohamed [26] studied the Soret effects on double-diffusive convection-radiation interaction on unsteady MHD flow over a vertical moving plate with heat generation. Devi and Raj [27] discussed thermodiffusion effects on unsteady hydromagnetic free convection flows with heat and mass transfer past a moving vertical plate with time-dependent suction and heat source in a slip regime. Pal and Talukdar [28, 29] analyzed the thermodiffusion effect on MHD flow through the vertical surface. The research works [30–32] scrutinized the thermodiffusion effect on unsteady MHD flow over a moving vertical porous surface. Ali et al. [33] inspected the Soret–Dufour effect on the hydromagnetic flow of viscoelastic fluid over a porous oscillatory stretching sheet in the presence of thermal radiation. Pal and Biswas [34] studied the Soret effects on chemically reacting mixed convection MHD oscillatory flow of Casson fluid with thermal radiation and viscous dissipation. Kataria and Patel [35] investigated the Soret effects on the heat-generating MHD Casson fluid flow past an oscillating vertical plate embedded in a porous medium. Prabhakar Reddy and Sunzu [36] inspected Dufour and Soret effects on unsteady MHD-free convective flow of viscous incompressible fluid past an infinite vertical porous plate in the presence of radiation. Prabhakar Reddy [37] investigated thermodiffusion effects on radiating and reacting MHD convective heat-absorbing fluid past an exponentially accelerated vertical porous plate with ramped temperature in the presence of Hall current. Prabhakar Reddy and Hugo [38] discussed the Soret effect on radiating and reacting unsteady MHD flow past an exponentially accelerated inclined porous plate.

Therefore, all the abovementioned studies forced us to conduct the study of MHD unsteady-free convective flow past an exponentially accelerated inclined permeable plate embedded in a saturated porous medium of uniform permeability in the presence of chemical reaction, radiation, and thermodiffusion effects as this study is not being discussed yet. This kind of problem is essential in the areas of nuclear power plants, MHD pumps, food processing, polymer production, and also in the processes of isotope separation of medium molecular weighted gases (N_2, air) and mixture between gases with very light molecular weight (H_2, He). The main goal of this investigation is to fill the gap by extending the earlier published work of Pattnaik et al. [3], especially by incorporating thermodiffusion effect, which should increase the applicability of the study that constitutes the novelty of the current work.

2. Mathematical Analysis

We consider an unsteady MHD radiating-free convective flow of a viscous, incompressible fluid past an exponentially accelerated inclined plate embedded in a saturated porous medium with variable temperature and concentration, considering the thermodiffusion effect. In the coordinate system, the x' axis is taken along the plate, and the y' axis is taken normal to the plate. The plate is inclined to a vertical direction by an angle $(\circ)\lambda$, as shown in Figure 1. A uniform magnetic field of strength B_0 is applied in the direction normal to the plate. Initially, the plate and surrounding fluid are at the same temperature T_∞' and concentration C_∞'. At the time $t' > 0$, the temperature and species concentration level are raised or lowered linearly with time t' and the plate is exponentially accelerated with a velocity $u' = u_0 \exp(a't')$ in its plane. A homogeneous first-order chemical reaction rate is applied between the diffusing species and the fluid. The magnetic Reynolds number of the flow is minimal, so the induced magnetic field is ignored. Following the suggestions by Kumar and Varma [1] and Pattnaik et al. [3], the equations of momentum, energy, and species concentration of the flow under the usual boundary layer approximations are given by the following expressions:

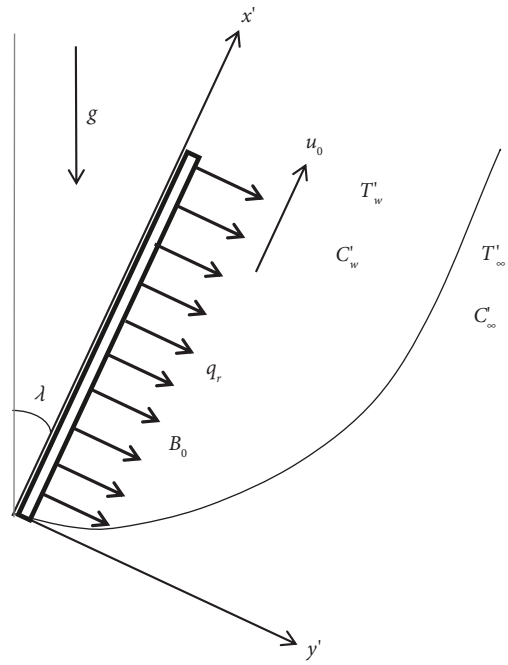

Figure 1: Physical sketch of the model.

$$\frac{\partial u^{'}}{\partial t^{'}} = \upsilon \frac{\partial^2 u^{'}}{\partial y'^2} + g\beta\left(T^{'} - T_{\infty}^{'}\right)\cos\lambda + g\beta^{*}\left(C^{'} - C_{\infty}^{'}\right)\cos\lambda - \frac{\sigma B_0^2 u^{'}}{\rho}, \tag{1}$$

$$\rho c_p \frac{\partial T^{'}}{\partial t^{'}} = k\frac{\partial^2 T^{'}}{\partial y'^2} - \frac{\partial q_r}{\partial y^{'}} + S^{'}\left(T^{'} - T_{\infty}^{'}\right), \tag{2}$$

$$\frac{\partial C^{'}}{\partial t^{'}} = D_m \frac{\partial^2 C^{'}}{\partial y'^2} + \frac{D_m K_T}{T_m}\left(\frac{\partial^2 T^{'}}{\partial y'^2}\right) - k_r^{'}\left(C^{'} - C_{\infty}^{'}\right). \tag{3}$$

The associated initial and boundary conditions are as follows:

$$\begin{aligned} &t^{'} \le 0; u^{'} = 0,\\ &T^{'} = T_{\infty}^{'},\\ &C^{'} = C_{\infty}^{'} \forall y^{'},\\ &t^{'} > 0; u^{'} = u_0 \exp\left(a^{'} t^{'}\right),\\ &T' = T_{\infty}^{'} + \left(T_w^{'} - T_{\infty}^{'}\right)\frac{u_0^2 t^{'}}{\upsilon},\\ &C' = C_{\infty}^{'} + \left(C_w^{'} - C_{\infty}^{'}\right)\frac{u_0^2 t^{'}}{\upsilon} \text{ at } y^{'} = 0,\\ &u^{'} = 0,\\ &T^{'} = T_{\infty}^{'},\\ &C^{'} = C_{\infty}^{'} \text{ as } y^{'} \longrightarrow \infty. \end{aligned} \tag{4}$$

Here, $u^{'}$ indicates fluid velocity (ms^{-1}), g indicates acceleration due to gravity (ms^{-2}), $T^{'}$ indicates fluid temperature (K), $T_w^{'}$ indicates constant temperature of the plate (K), $T_{\infty}^{'}$ indicates temperature of the fluid far away from the plate (K), $C^{'}$ indicates fluid concentration (kgm^{-3}), $C_w^{'}$ indicates concentration of the fluid near the plate (kgm^{-3}), $C_{\infty}^{'}$ indicates concentration of the fluid far away from the plate (kgm^{-3}), β indicates volumetric coefficient of thermal expansion (K^{-1}), β^{*} indicates volumetric coefficient of concentration expansion $(m^3 kg^{-1})$, B_0 indicates magnetic induction (Am^{-1}), $K_p^{'}$ indicates permeability of the porous medium, $S^{'}$ indicates constant heat source, k indicates thermal conductivity $(Wm^{-1}K^{-1})$, υ indicates kinematic viscosity $(m^2 s^{-1})$, μ indicates fluid viscosity $(kg/m^{-1}s^{-1})$, ρ indicates fluid density (kg/m^3), σ indicates electrical conductivity (S/m), c_p indicates specific heat at constant pressure $(Jkg^{-1}k)$, q_r indicates radiation heat flux (W/m^2), $k_r^{'}$ indicates chemical reaction constant, D_m indicates chemical molecular diffusivity $(m^2 s^{-1})$, T_m indicates mean fluid temperature, K_T indicates thermal diffusion ratio, $a^{'}$ indicates accelerating parameter, and $t^{'}$ indicates time (s).

The fluid is considered a gray, absorbing-emitting radiation but a nonscattering medium in the analysis. The local gradient for the case of an optically thin gray gas following the study by England and Emery [39] is expressed as follows:

$$q_r = -a^{*}\sigma\left(T_{\infty}^{'4} - T^{'4}\right), \tag{5}$$

where σ and a^{*} are, respectively, the Stefan–Boltzmann constant and absorption coefficient. Assuming slight temperature differences within the flow, the term $T^{'4}$ is expressed as the linear function of temperature. Using the Taylor series, expanding $T^{'4}$ about a free stream temperature

T_∞' and neglecting higher order terms, we obtain the following expression:

$$T'^4 \simeq 4T'^3_\infty T' - 3T'^4_\infty. \tag{6}$$

On substitution of equations (5) and (6) in equation (2), the energy equation becomes as follows:

$$\rho c_p \frac{\partial T'}{\partial t'} = k\frac{\partial^2 T'}{\partial y'^2} - 16a^*\sigma T'^3_\infty\left(T' - T_\infty'\right) + S'\left(T' - T_\infty'\right). \tag{7}$$

On introducing the following nondimensional quantities and parameters

$$u = \frac{u'}{u_0},$$

$$\tau = \frac{t' u_0^2}{v},$$

$$\eta = \frac{y' u_0}{v},$$

$$a = \frac{a' v}{u_0^2},$$

$$S_c = \frac{v}{D_m},$$

$$P_r = \frac{\mu c_p}{k},$$

$$M = \frac{\sigma B_0^2 v}{\rho u_0^2},$$

$$\gamma = \frac{v k_r'}{u_0^2},$$

$$S = \frac{S' v}{\rho c_p u_0^2},$$

$$K_p = \frac{u_0^2 K_p'}{v},$$

$$\theta = \frac{T' - T_w'}{T_w' - T_\infty'},$$

$$\phi = \frac{C' - C_w'}{C_w' - C_\infty'},$$

$$G_r = \frac{g\beta v\left(T' - T_\infty'\right)}{u_0^3},$$

$$G_m = \frac{g\beta^* v\left(C' - C_\infty'\right)}{u_0^3},$$

$$S_r = \frac{D_m K_T\left(T_w' - T_\infty'\right)}{v T_m\left(C_w' - C_\infty'\right)}, \text{ and}$$

$$R = \frac{16\sigma a^* v^2 T'^3_\infty}{k u_0^2}. \tag{8}$$

into equations (1), (3), (4), and (7), the following dimensionless governing coupled partial differential equations of the flow are obtained.

$$\frac{\partial u}{\partial \tau} = \frac{\partial^2 u}{\partial \eta^2} + G_r\theta\cos\lambda + G_m\phi\cos\lambda - Mu - \frac{u}{K_p}, \tag{9}$$

$$\frac{\partial \theta}{\partial \tau} = \frac{1}{P_r}\frac{\partial^2 \theta}{\partial \eta^2} - \frac{R}{P_r}\theta + S\theta, \tag{10}$$

$$\frac{\partial \phi}{\partial \tau} = \frac{1}{S_c}\frac{\partial \phi}{\partial \eta^2} + S_r\left(\frac{\partial^2 \theta}{\partial \eta^2}\right) - \gamma\phi. \tag{11}$$

The corresponding initial and boundary conditions in a dimensionless form become as follows:

$$\begin{aligned}
&\tau \le 0\text{: } u = 0,\\
&\theta = 0,\\
&\phi = 0 \text{ for all } \eta,\\
&\tau > 0\text{: } u = \exp(a\tau),\\
&\theta = \tau,\\
&\phi = \tau \text{ at } \eta = 0,\\
&u \longrightarrow 0,\\
&\theta \longrightarrow 0,\\
&\phi \longrightarrow 0 \text{ as } \eta \longrightarrow \infty.
\end{aligned} \tag{12}$$

3. Numerical Procedure

The constructing coupled nonlinear partial differential equations of the model equations (9)–(11) subject to the initial and boundary conditions (12) have been solved numerically via DuFort–Frankel's explicit finite difference method given in the study by Jain et al. [40], which is unconditionally stable. The corresponding finite difference equations to the equations (9)–(11) are derived as follows:

$$\left(\frac{u_{i,j+1}-u_{i,j-1}}{2\Delta\tau}\right)=\left(\frac{u_{i-1,j}-u_{i,j+1}-u_{i,j-1}+u_{i+1,j}}{(\Delta\eta)^2}\right)-\frac{1}{2}\left(M+\frac{1}{K_p}\right)\left(u_{i,j+1}+u_{i,j-1}\right)+\frac{1}{2}G_r\left(\theta_{i,j+1}+\theta_{i,j-1}\right)\cos\lambda+\frac{1}{2}G_m\left(\phi_{i,j+1}+\phi_{i,j-1}\right)\cos\lambda, \tag{13}$$

$$\left(\frac{\theta_{i,j+1}-\theta_{i,j-1}}{2\Delta\tau}\right)=\frac{1}{P_r}\left(\frac{\theta_{i-1,j}-\theta_{i,j+1}-\theta_{i,j-1}+\theta_{i+1,j}}{(\Delta\eta)^2}\right)-\frac{R}{2P_r}\left(\theta_{i,j+1}+\theta_{i,j-1}\right)+\frac{S}{2}\left(\theta_{i,j+1}+\theta_{i,j-1}\right), \tag{14}$$

$$\left(\frac{\phi_{i,j+1}-\phi_{i,j-1}}{2\Delta\tau}\right)=\frac{1}{S_c}\left(\frac{\phi_{i-1,j}-\phi_{i,j+1}-\phi_{i,j-1}+\phi_{i+1,j}}{(\Delta\eta)^2}\right)+S_r\left(\frac{\theta_{i-1,j}-\theta_{i,j+1}-\theta_{i,j-1}+\theta_{i+1,j}}{(\Delta\eta)^2}\right)-\frac{\gamma}{2}\left(\phi_{i,j+1}+\phi_{i,j-1}\right). \tag{15}$$

The initial and boundary conditions (13) become as follows:

$$\begin{aligned}
u_{i,0} &= 0,\\
\theta_{i,0} &= 0,\\
\phi_{i,0} &= 0, \text{for all } i\\
u_{0,j} &= \exp(at),\\
\theta_{0,j} &= j\Delta\tau,\\
\phi_{0,j} &= j\Delta\tau,\\
u_{\max,j} &\longrightarrow 0,\\
\theta_{\max,j} &\longrightarrow 0,\\
\phi_{\max,j} &\longrightarrow 0.
\end{aligned} \tag{16}$$

Here, max corresponds to infinite. The suffix i corresponds to space η and the suffix j corresponds to time τ. Also, $\Delta\eta=\eta_{i+1}-\eta_i$ and $\Delta\tau=\tau_{i+1}-\tau_i$. The region of integration of the problem is considered as a rectangle with sides $\tau_{\max}=2$ and $\eta_{\max}=4$ where $\eta_{\max}$ corresponds to $(\eta=\infty)$; this has been done after some numerical experimentation. A value greater than 4 does not result in any significant change in the numerical results. Numerical results of the velocity $u(\eta,\tau)$, temperature $\theta(\eta,\tau)$, and concentration $\phi(\eta,\tau)$ are obtained from equations (13)–(15) under the initial and boundary conditions (16). The grid size $\Delta\eta=0.1$ along $\eta-$ direction and $\Delta\tau=0.002$ along $\tau-$ direction was selected after some numerical experimentation with grid seizes $\Delta\tau=0.001$ and 0.0025; no significant change in the results was noticed. To verify the accuracy of the present numerical scheme, a comparison of the computed Nusselt number in the present work was made with that of the Nusselt number obtained by the Laplace transform technique in the earlier published work of Pattnaik et al. [3] shown in Table 1; a perfect agreement was achieved. This verifies the accuracy of the present numerical scheme.

4. Results and Discussion

To evaluate the physical significance of the problem, numerical calculations were made for different values of thermophysical parameters controlling the flow, such as magnetic parameter M, permeability parameter K_p, inclination of angle λ, plate acceleration a, radiation parameter R, heat source parameter S, thermodiffusion parameter S_r, chemical reaction rate γ, and time τ, which are displayed through the graphs and tables to analyze the variations of velocity, temperature, concentration profiles, skin friction, and Nusselt and Sherwood numbers. We set default values of critical parameters as $G_r=10$, $G_m=5$, $M=5$, $K_p=0.5$, $P_r=0.71$, $R=4$, $S=2$, $S_c=0.6$, $S_r=2$, $\gamma=0.2$, $\lambda=\pi/6$, $a=0.5$, and $\tau=0.4$ in all figures and tables unless specified.

Figure 2 illustrates the effect of magnetic parameter M and porosity parameter K_p on velocity profiles against η. It is seen from Figure 2(a) that an increase in the magnetic field intensity leads to a decrease in the fluid motion. Physically, increasing values of M generates resistive forces strong enough so that they can oppose the fluid motion, and as a result, fluid velocity decreases. Also, it is observed that there is a sudden rise in the fluid velocity near the plate in the absence of a magnetic field. In Figure 2(b), the reverse impact on the fluid velocity to that of the magnetic field is seen. This is due to the fact that uprising values of K_p reduce the drag force; as a result, they increase the fluid momentum. Figure 3 depicts the variation of the velocity profiles against η for various values of angle of inclination λ and acceleration parameter a. It is observed from Figure 3(a) that an increasing angle of inclination reduces the fluid velocity due to forcing forces being drained due to the factor $\cos\lambda$. It is noticed from Figure 3(b) that the fluid momentum improves with increasing acceleration parameter. Also, it is clear that when $a=0$ the case of constant plate velocity and satisfies the boundary condition $(u=1)$ implies that a thinner boundary layer. The variation of velocity and temperature profiles under the effects of the thermal radiation parameter R against η is shown in Figure 4. It is perceived that both fluid velocity and temperature deflate with the expansion of the radiation parameter. Physically, when radiation is presented in the energy equation, the thermal boundary layer is always starting to thicken; as a result, fluid temperature diminishes and the speed of velocity is lower. The impact of the heat source/sink parameter S on the velocity and temperature profiles against η is displayed in Figure 5. It is found that fluid velocity, as well as temperature, amplifies with

Table 1: Comparison of Nusselt number N_u.

P_r	R	S	τ	Results of Pattnaik et al. [3]	Present results
0.71	4	2	0.2	0.5214	0.5215
0.5	4	2	0.2	0.4849	0.4849
0.5	10	2	0.2	0.6832	0.6831
0.71	4	7	0.2	0.4629	0.4629
0.71	4	−2	0.2	0.6145	0.6145
0.71	4	2	0.5	1.0208	1.0208

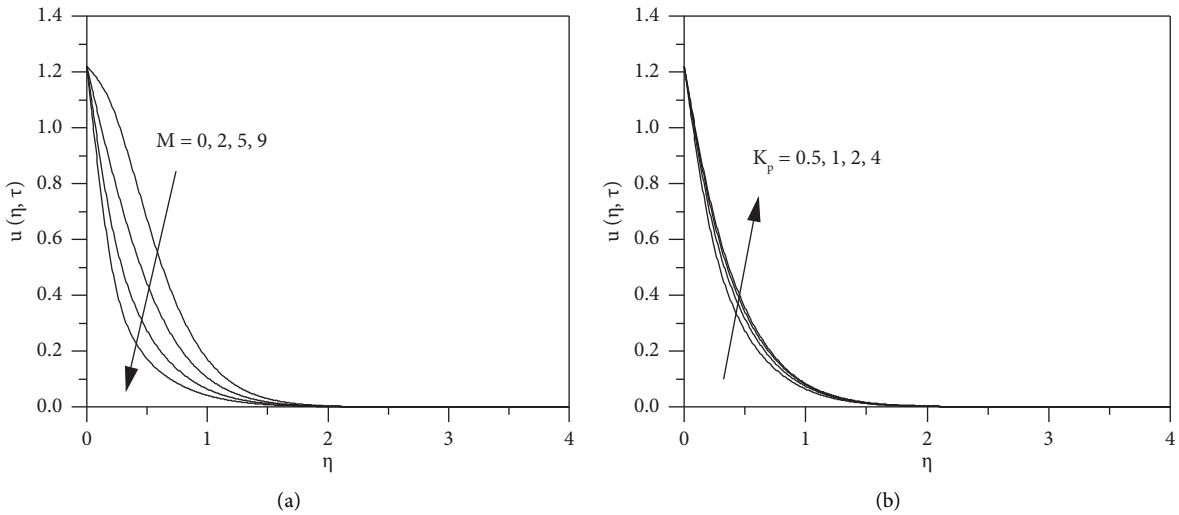

Figure 2: Variation of velocity profiles against η for different values of (a) M and (b) K_p.

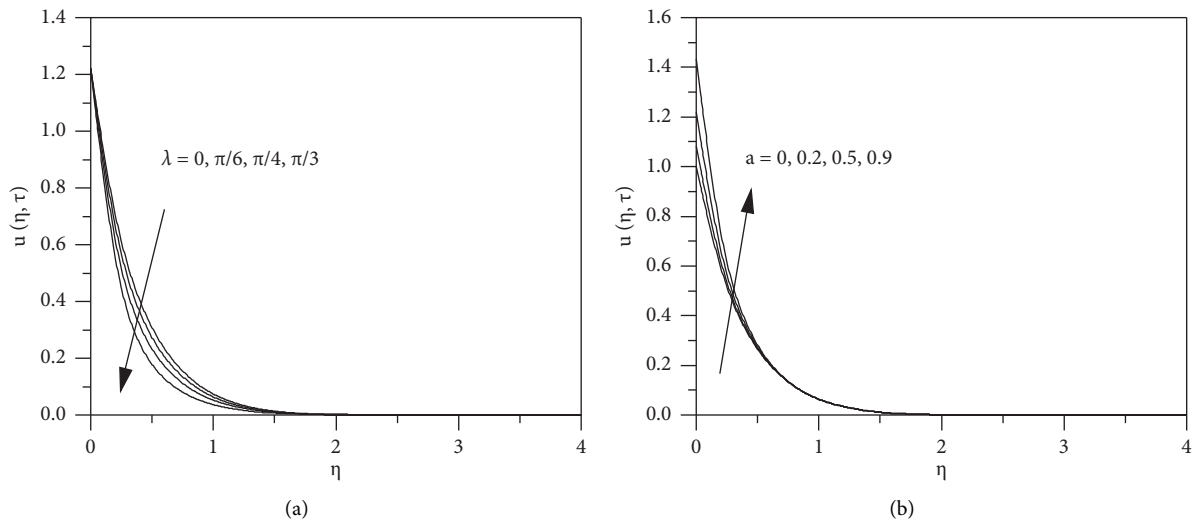

Figure 3: Variation of velocity profiles against η for different values of (a) λ and (b) a.

growing heat source ($S > 0$) parameter, whilst the overturn is noted in the case of heat sink ($S < 0$). Physically, more heat is generated from the surface to the fluid when increasing values of heat source parameter, as a result, enhanced fluid temperature consequently boost up fluid velocity whilst when heat sink present in the boundary layer, engross energy, which causes to reduce the fluid temperature as a consequence slowdown fluid flow. Figure 6 illustrates the effects of the thermodiffusion parameter S_r on the velocity and concentration profiles against η. It can be seen that an

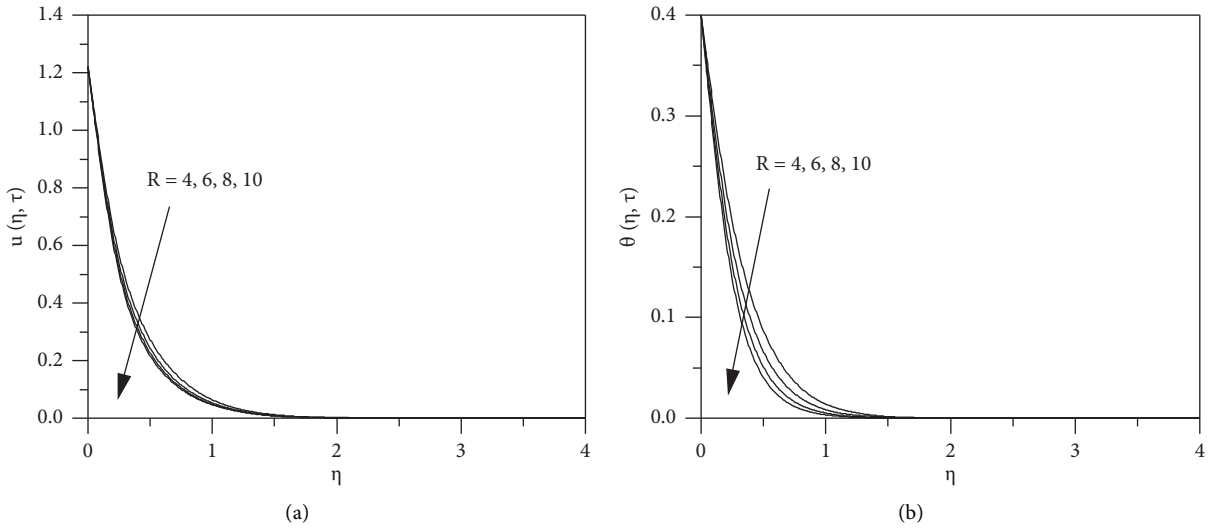

Figure 4: Variation of (a) velocity profiles and (b) temperature profiles against η for different values of R.

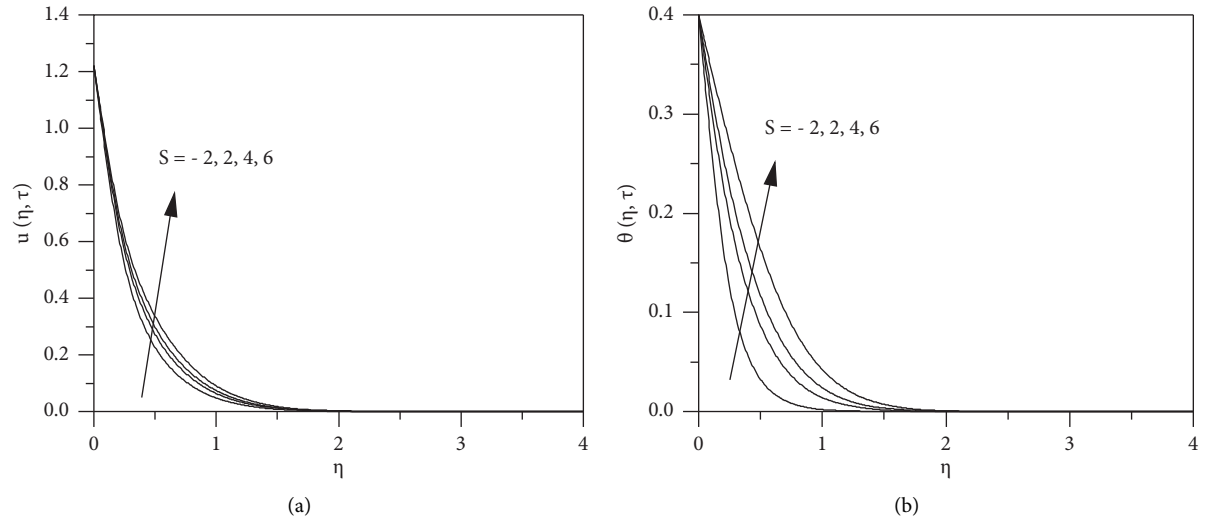

Figure 5: Variation of (a) velocity profiles and (b) temperature profiles against η for different values of S.

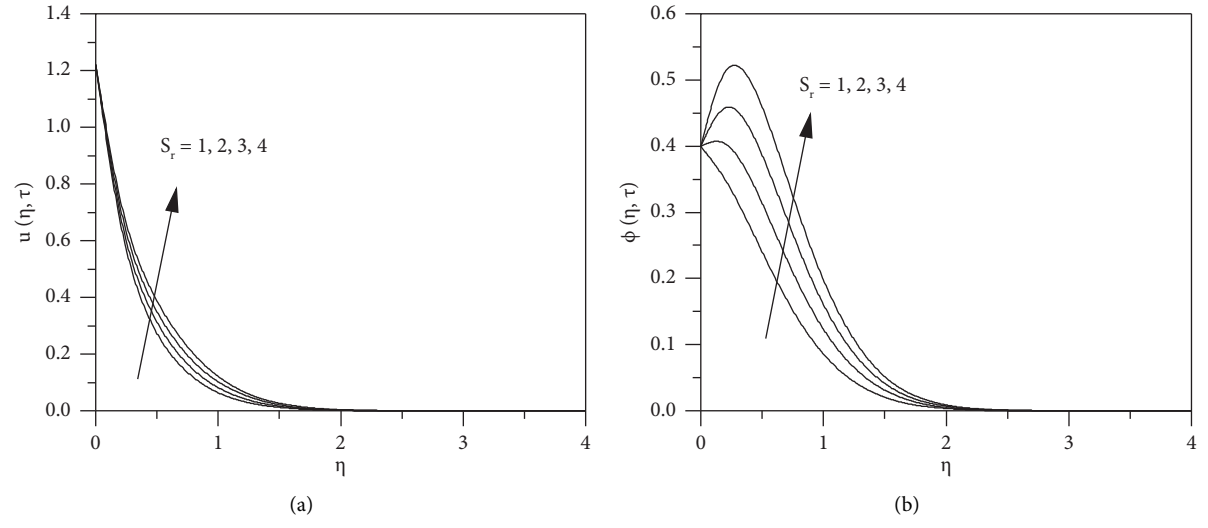

Figure 6: Variation of (a) velocity profiles and (b) concentration profiles against η for different values of S_r.

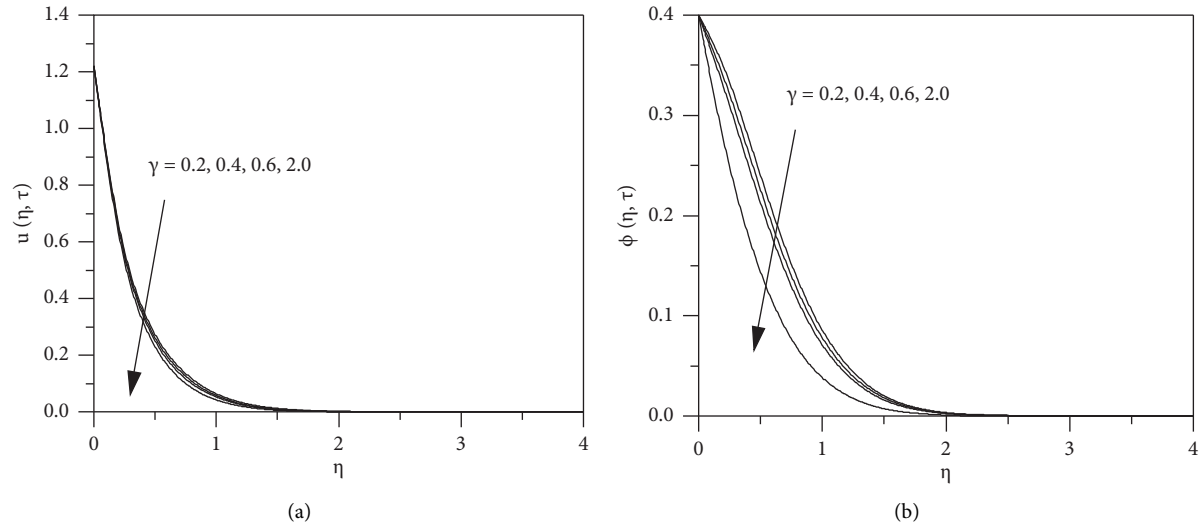

Figure 7: Variation of (a) velocity profiles and (b) concentration profiles against η for different values of γ.

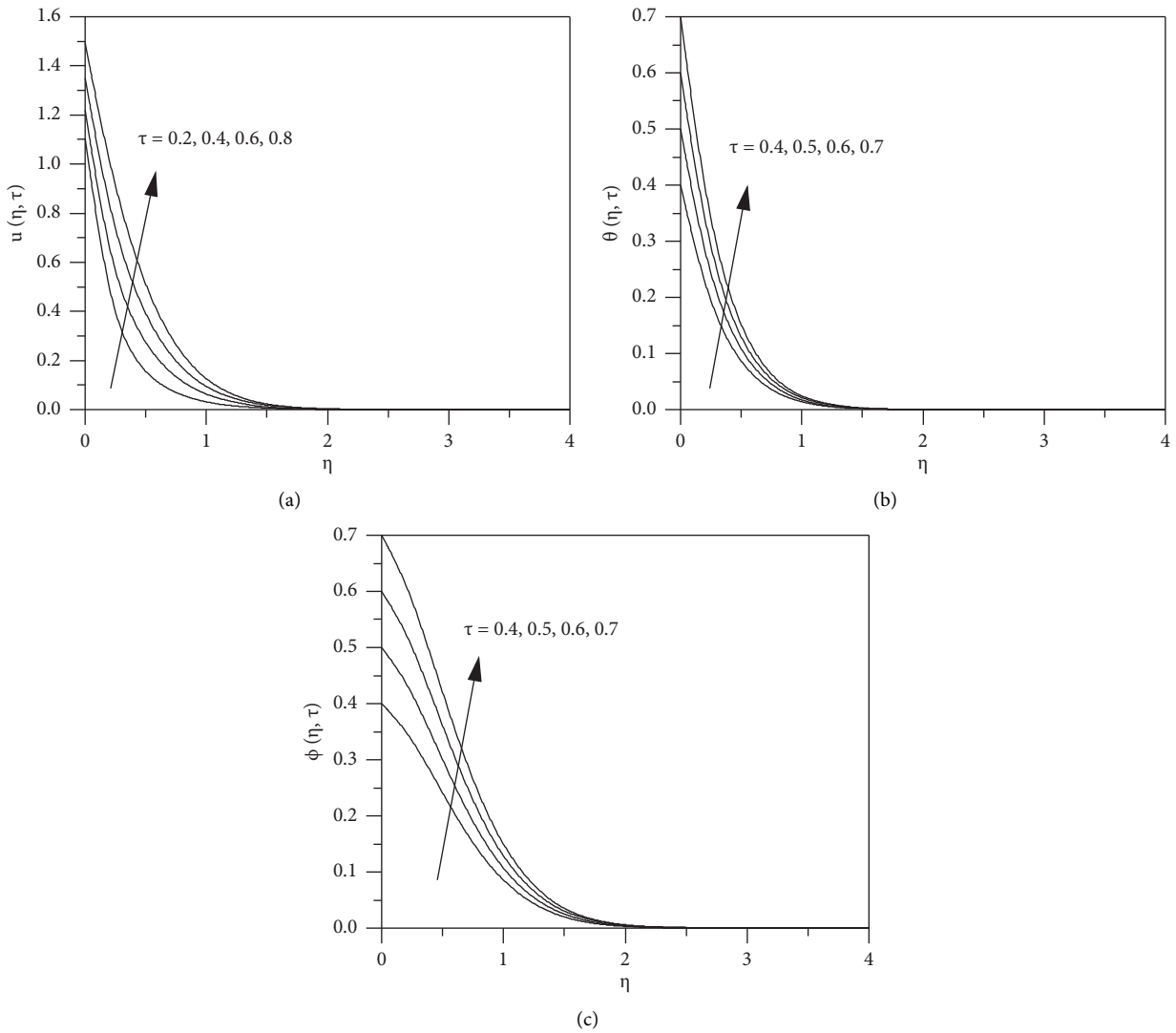

Figure 8: Variation of (a) velocity profiles, (b) temperature profiles, and (c) concentration profiles against η for different values of τ.

Table 2: Variation of skin friction.

G_r	G_m	M	K_p	λ (degrees)	P_r	R	S	a	C_f
10	5	5	0.5	30	0.71	4	2	0.5	1.229278
15									1.051202
	10								0.924504
		2							0.737566
			1.0						1.089258
				60					1.495236
					0.5				1.187518
						6			1.286034
							4		1.115942
							−2		1.327122
								0.2	1.012248

Table 3: Variation of skin friction and Sherwood number.

S_c	S_r	γ	τ	C_f	S_h
0.6	1	0.2	0.4	1.229278	0.550884
3.0				1.250034	1.197680
	2			1.164052	–0.197040
		2.0		1.295908	0.764372
			0.6	1.098086	0.826320

increasing behavior in both fluid velocity and concentration with rising values of S_r. Physically, increasing the thermodiffusion effect tends to raise mass buoyancy force, which results in an increase of species concentration as outcome growth flow transports in the boundary layer. The variation of velocity and concentration profiles for various values of chemical reaction parameter γ against η is depicted in Figure 7. This indicates that the destructive chemical reaction rate $\gamma > 0$ leads to descending both fluid velocity and concentration, which is a physical reality. Since an increase in γ weakens the buoyancy effects in the boundary layer due to concentration gradients, both velocity and concentration decrease. Figure 8 demonstrates the variation of velocity, temperature, and concentration profiles under the variation of time τ against η. It is observed from Figure 8(a) that an increasing effect on the fluid velocity with time progression due to increasing buoyancy effect causes to enhance momentum boundary layer thickness. It is noticed from Figures 8(b) and 8(c) that both fluid temperature and concentration enhance in the boundary layer on escalating values of τ. Further initially, the plate temperature and concentrations are equal to the time, and for larger values of $\eta\,(\eta > 0)$, both tend to zero with growing values of time τ, which is a clear validation of the thermal and concentration boundary conditions.

From Table 1, it is perceived that the Nusselt number at the plate surface increases with an increase in Prandtl number, radiation parameter, and time, whereas it decreases with an increase in heat source parameter. The presence of a heat sink clearly supports the appreciation of the Nusselt number. From Tables 2 and 3, it is seen that the skin friction at the plate surface decreases with an enhancement in permeability parameter, heat source parameter, thermodiffusion parameter, time, thermal, and mass buoyancy forces, whereas it increases with an increase in magnetic parameter, inclination of angle, Prandtl number, radiation parameter, acceleration parameter, Schmidt number, and chemical reaction parameter. Also, it is clear that heat sink helps to improve the skin friction. It is observed from Table 3 that an increase in Schmidt number, chemical reaction rate, and time increases the Sherwood number at the plate surface, whereas it decreases with an increase in the thermodiffusion parameter.

5. Conclusions

The governing coupled nonlinear partial differential equations of the problem are solved numerically by the finite difference method to analyze the effects of thermodiffusion and chemical reaction on magnetohydrodynamic unsteady-free convective flow past an exponentially accelerated inclined permeable plate embedded in a porous medium in the presence of radiation and heat source/sink. We found that magnetic field force and angle of inclination decelerate fluid motion, whereas a reverse trend is noted with enhancement in porosity parameter, plate acceleration, and time. The fluid velocity and temperature increase with the growing heat source parameter, whereas radiation and heat sink have overturned fluid velocity and temperature results. The thermodiffusion effect enhances fluid velocity and concentration, whereas the chemical reaction rate has a reverse impact. Thermal and mass buoyancy forces, heat source, the permeability of the medium, and time tend to lessen the skin friction, whereas magnetic field, angle of inclination, radiation, chemical reaction rate, and plate acceleration tend to raise the skin friction. The Nusselt number increases with

increasing radiation parameters, heat sink, and time at the plate surface, whereas the heat source has the opposite effect. An increase in the Schmidt number and chemical reaction rate helps to raise the Sherwood number, whereas the thermodiffusion effect has the opposite tendency.

Data Availability

The authors confirm that the data supporting the findings of this research are available within the article.

Disclosure

Preprint Source: https://www.authorea.com/doi/full/10.22541/au.164865092.20993641.

Conflicts of Interest

The authors declare that they have no conflicts of interest.

Acknowledgments

The authors are thankful to the management of the University of Dodoma, Tanzania, for their constant encouragement.

References

[1] A. G. V. Kumar and S. V. K. Varma, "Radiation effects on MHD flow past an impulsively started exponentially accelerated vertical plate with variable temperature in the presence of heat generation," *International Journal of Engineering Science and Technology*, vol. 3, no. 4, pp. 2897–2909, 2011.

[2] R. Nandkeolyar, G. S. Seth, O. D. Makinde, P. Sibanda, and M. S. Ansari, "Unsteady hydro-magnetic natural convection flow of a dusty fluid past an impulsively moving vertical plate with ramped temperature in the presence of thermal radiation," *Journal of Applied Mechanics*, vol. 80, no. 6, Article ID 061003, 2013.

[3] J. R. Pattnaik, G. C. Dash, and S. Singh, "Radiation and mass transfer effects on MHD flow through porous medium past an exponentially accelerated inclined plate with variable temperature," *Ain Shams Engineering Journal*, vol. 8, no. 1, pp. 67–75, 2017.

[4] M. Veera Krishna, G. Subba Reddy, and A. J. Chamkha, "Hall effects on unsteady MHD oscillatory free convective flow of second-grade fluid through porous medium between two vertical plates," *Physics of Fluids*, vol. 30, no. 2, Article ID 023106, 2018.

[5] H. R. Patel, A. S. Mittal, and R. R. Darji, "MHD flow of micropolar nanofluid over a stretching/shrinking sheet considering radiation," *International Communications in Heat and Mass Transfer*, vol. 108, Article ID 104322, 2019.

[6] A. S. Mittal, H. R. Patel, and R. R. Darji, "Mixed convection micropolar ferrofluid flow with viscous dissipation, joule heating and convective boundary conditions," *International Communications in Heat and Mass Transfer*, vol. 108, Article ID 104320, 2019.

[7] A. S. Mittal, "Analysis of water-based composite MHD fluid flow using HAM," *International Journal of Ambient Energy*, vol. 42, no. 13, pp. 1538–1550, 2019.

[8] A. S. Mittal, "Study of radiation effects on unsteady 2D MHD Al2O3-water flow through parallel squeezing plates," *International Journal of Ambient Energy*, vol. 43, no. 1, pp. 653–660, 2019.

[9] M. Veera Krishna, N. Ameer Ahamad, and A. J. Chamkha, "Hall and ion slip effects on unsteady MHD free convective rotating flow through a saturated porous medium over an exponential accelerated plate," *Alexandria Engineering Journal*, vol. 59, no. 2, pp. 565–577, 2020.

[10] M. Veera Krishna, K. Jyothi, and A. J. Chamkha, "Heat and mass transfer on MHD flow of second-grade fluid through porous medium over a semi-infinite vertical stretching sheet," *Journal of Porous Media*, vol. 23, no. 8, pp. 751–765, 2020.

[11] M. Veera Krishna, N. Ameer Ahamad, and A. J. Chamkha, "Radiation absorption on MHD convective flow of nanofluids through vertically travelling absorbent plate," *Ain Shams Engineering Journal*, vol. 12, no. 3, pp. 3043–3056, 2021.

[12] M. Veera Krishna, N. Ameer Ahamad, and A. F. Aljohani, "Thermal radiation, chemical reaction, Hall and ion slip effects on MHD oscillatory rotating flow of micro-polar liquid," *Alexandria Engineering Journal*, vol. 60, no. 3, pp. 3467–3484, 2021.

[13] V. Sugunamma, N. Sandeep, P. M. Veera Krishna, and R. Bahunadam, "Inclined magnetic field and chemical reaction effects on flow over a semi-infinite vertical porous plate through porous medium," *Comm. Appl. Sci*, vol. 1, no. 1, pp. 1–24, 2013.

[14] F. Ali, I. Khan, S. Shafie, and N. Musthapa, "Heat and mass transfer with free convection MHD flow past a vertical plate embedded in porous medium," *Mathematical Problems in Engineering*, vol. 2013, Article ID 346281, 13 pages, 2013.

[15] A. Mythreye, J. Pramod, and K. S. Balamurugan, "Chemical reaction on unsteady MHD convective heat and mass transfer past a semi-infinite vertical permeable moving plate with heat absorption," *Procedia Engineering*, vol. 127, pp. 613–620, 2015.

[16] G. S. Seth and S. Sarkar, "Hydro-magnetic natural convection flow with induced magnetic field and nth-order chemical reaction of a heat absorbing fluid past an impulsively moving vertical plate with ramped temperature," *Bulgarian Chemical Communications*, vol. 47, no. 1, pp. 66–79, 2015.

[17] R. S. Tripathy, G. C. Dash, S. R. Mishra, and S. Baag, "Chemical reaction effect on MHD free convective surface over a moving vertical plate through porous medium," *Alexandria Engineering Journal*, vol. 54, no. 3, pp. 673–679, 2015.

[18] S. Agarwalla and N. Ahmed, "MHD mass transfer flow past an inclined plate with variable temperature and plate velocity embedded in a porous medium," *Heat Transfer - Asian Research*, vol. 47, no. 1, pp. 27–41, 2018.

[19] M. Veera Krishna and A. J. Chamkha, "Hall effects on unsteady MHD flow of second-grade fluid through porous medium with ramped wall temperature and ramped surface concentration," *Physics of Fluids*, vol. 30, no. 5, Article ID 053101, 2018.

[20] M. Veera Krishna and A. J. Chamkha, "Hall and ion slip effects on MHD rotating boundary layer flow of nanofluid past an infinite vertical plate embedded in a porous medium," *Results in Physics*, vol. 15, Article ID 102652, 2019.

[21] M. Veera Krishna, P. V. S. Anand, and A. J. Chamkha, "Heat and mass transfer on free convective flow of a micro-polar fluid through a porous surface with inclined magnetic field and Hall effects," *Special Topics and Reviews in Porous Media - An International Journal*, vol. 10, no. 3, pp. 203–223, 2019.

[22] B. Reddy, "Effects of chemical reaction on transient MHD flow with mass transfer past an impulsively fixed infinite vertical plate in the presence of thermal radiation," *International Journal of Applied Mechanics and Engineering*, vol. 24, no. 4, pp. 169–182, 2019.

[23] M. V. Krishna and A. J. Chamkha, "Hall and ion slip effects on MHD rotating flow of elastico-viscous fluid through porous medium," *International Communications in Heat and Mass Transfer*, vol. 113, Article ID 104494, 2020.

[24] M. V. Krishna, N. A. Ahammad, and A. J. Chamkha, "Radiative MHD flow of Casson hybrid nanofluid over an infinite exponentially accelerated vertical porous surface," *Case Studies in Thermal Engineering*, vol. 27, Article ID 101229, 2021.

[25] M. Veera Krishna, N. Ameer Ahamad, and A. J. Chamkha, "Hall and ion slip impacts on unsteady MHD convective rotating flow of heat generating/absorbing second-grade fluid," *Alexandria Engineering Journal*, vol. 60, no. 1, pp. 845–858, 2021.

[26] R. A. Mohamed, "Double-diffusive convection-radiation interaction on unsteady MHD flow over a vertical moving plate with heat generation and Soret effects," *Applied Mathematical Sciences*, vol. 13, no. 3, pp. 629–651, 2009.

[27] S. P. A. Devi and J. W. S. Raj, "Thermo-diffusion effects on unsteady hydro-magnetic free convection flow with heat and mass transfer past a moving vertical plate with time-dependent suction and heat source in a slip regime," *International Journal of Applied Mathematics and Mechanics*, vol. 7, pp. 20–25, 2011.

[28] D. Pal and B. Talukdar, "Influence of fluctuating thermal and mass diffusion on unsteady MHD buoyancy-driven convection past a vertical surface with chemical reaction and Soret effects," *Communications in Nonlinear Science and Numerical Simulation*, vol. 17, no. 4, pp. 1597–1614, 2012.

[29] D. Pal and B. Talukdar, "Influence of Soret effect on MHD mixed convection oscillatory flow over a vertical surface in a porous medium with chemical reaction and thermal radiation," *International Journal of Nonlinear Science*, vol. 14, no. 1, pp. 65–78, 2012.

[30] T. S. Reddy, S. M. Ibrahim, A. S. Reddy, and P. Raju, "Double-diffusive convection- radiation interaction on unsteady MHD flow of a micro-polar fluid over a vertical moving plate embedded in a porous medium with chemical reaction and Soret effects," *Journal of Global Research in Mathematical Archives*, vol. 7, no. 1, pp. 72–87, 2013.

[31] B. M. Rao, G. V. Reddy, M. C. Raju, and S. V. K. Varma, "Unsteady MHD free convection heat and mass transfer flow past a semi-infinite vertical permeable moving with heat absorption, radiation, chemical reaction and Soret effects," *International Journal of Engineering Sciences and Emerging Technologies,* vol. 2, no. 6, pp. 241–257, 2013.

[32] G. S. Seth, B. Kumbhakar, and S. Sarkar, "Soret and Hall effects on unsteady MHD free convection flow of radiating and chemically reactive fluid past a moving vertical plate with ramped temperature in rotating system," *International Journal of Engineering, Science and Technology*, vol. 7, no. 2, pp. 94–108, 1970.

[33] N. Ali, S. U. Khan, Z. Abbas, and M. Sajid, "Soret and Dufour effects on hydromagnetic flow of viscoelastic fluid over porous oscillatory stretching sheet with thermal radiation," *Journal of the Brazilian Society of Mechanical Sciences and Engineering*, vol. 38, no. 8, pp. 2533–2546, 2016.

[34] D. Pal and S. Biswas, "Influence of chemical reaction and Soret effect on mixed convective MHD oscillatory flow of Casson fluid with thermal radiation and viscous dissipation," *International Journal of Algorithms, Computing and Mathematics*, vol. 3, pp. 1897–1919, 2016.

[35] H. Kataria and H. Patel, "Soret and heat generation effects on MHD Casson fluid flow past an oscillating vertical plate embedded through porous medium," *Alexandria Engineering Journal*, vol. 55, no. 3, pp. 2125–2137, 2016.

[36] B. Prabhakar Reddy and J. M Sunzu, "Dufour and Soret effects on unsteady MHD free convective flow of viscous incompressible fluid past an infinite vertical porous plate in the presence of radiation," *Journal of the Serbian Society for Computational Mechanics*, vol. 12, no. 1, pp. 9–26, 2018.

[37] B. Prabhakar Reddy, "Thermo-diffusion and Hall effect on radiating and reacting mhd convective heat absorbing fluid past an exponentially accelerated vertical porous plate with ramped temperature," *Journal of the Serbian Society for Computational Mechanics*, vol. 14, no. 1, pp. 12–28, 2020.

[38] B. Prabhakar Reddy and A. Hugo, "Radiating and reacting MHD unsteady flow past an exponentially accelerated inclined permeable plate in a porous medium with Soret effect," *Authorea, March*, vol. 30, 2022.

[39] W. G. England and A. F. Emery, "Thermal radiation effects on the laminar free convection boundary layer of an absorbing gas," *Journal of Heat Transfer*, vol. 91, no. 1, pp. 37–44, 1969.

[40] M. K. Jain, S. R. K. Iyengar, and R. K. Jain, *Computational Methods for Partial Differential Equations*, Wiley Eastern Limited, Hoboken, NJ, USA, 1994.